An approach for numerical validation of aerodynamic effects through thermography

M. MALERBA, M. ARGENTO, A. SALVIUOLO, G. L. ROSSI
Dipartimento di Ingegneria Industriale
Università degli Studi di Perugia
Via G. Duranti, 67 – 06125 Perugia (PG)
ITALY

Abstract: - In fluid-dynamic phenomena analisys the boundary layer plays a fundamental role It also affects the drag and lift force of a body immersed in a fluid. Reynolds analogy introduces the possibility to use high sensitivity thermographic systems. Such approaches can be used to analyse the distribution of shear stress on the surface of solid bodies immersed into a fluid through temperature distribution. Temperature field can be acquired with the aid of a thermographic system on the surface of a solid body invested by a flow. Temperature distribution depends on many combined effects, such as: conversion of kinetic energy of the flow into thermal energy, flow temperature variation in time and space, convection heat transfer phenomena between flow and body, conduction phenomena inside the body, and radiation heath exchange.
A numerical approach was used to validate the proposed procedure. A transient simulation with increasing inlet fluid temperature was carried out to evaluate the thermal exchange between the airstream and the body. The effect of the different thermal exchange due to the local flow peculiarity is modelled.

Key-Words: - boundary layer, infrared thermography, subsonic flow, passive technique, wing profile, CFD

Nomenclature

Nu	Nusselt number
Nu_x	Local Nusselt number
Re	Reynolds number
Re_x	Local Reynolds number
Pr	Prandl number
C_f	Surface shear stress coefficient
C_{fx}	Local surface shear stress coefficient
ν	Kinematic viscosity
h_x	Convective coefficient
Φ	Heat flux exchange
T_∞	Temperature of the fluid
T	Temperature of the body surface
ρ	Density
$\Phi_{cond.lat.}$	Thermic stream due to lateral conduction
Φ_j	Thermic stream due to Joule's effect
Φ_{rad}	Thermic stream due to radiation effect
e	Thickness

1 Introduction

In all aerodynamic aspects, known of boundary layer pattern plays a fundamental role on the analysis of fluid dynamic phenomena and on interaction between solid bodies and surrounding fluid flow. Systems based on high resolution thermographic visualization seems to be very interesting measurement techniques to monitoring it.

These systems detect temperature distribution of a body surface. Measurement principles adopted are based on the heat exchange that take place between a solid body and the surrounding fluid flow. In this situation, temperature pattern is due to three different phenomena: thermodynamic effects of fluid flow temperature change due to the friction, heat transmission phenomena by convection between flow and body and conduction phenomena inside the body. If we neglect conduction phenomenon, the energy associated with convection between body and fluid, can be described by [1]:

$$\Phi = h_x (T - T_\infty) \qquad (1)$$

where heat transfer coefficient h_x change both if the flow is laminar or turbulent [8-10].

If the body is moving across a fluid, a correlation between thermographic and fluid-dynamic pattern can be done. A well known hypothesis that permits this correlation is Reynold's analogy, expressed by the following relation [2]:

$$\frac{Nu_x}{\mathrm{Re}_x \cdot \mathrm{Pr}} = \frac{C_{fx}}{2} \qquad (2)$$

that can be also expressed as:

$$C_{fx} = 2 \cdot \frac{\nu \cdot h_x}{c \cdot k} \tag{3}$$

This equation correlates heat exchange coefficient h_x and local surface shear stress coefficient C_{fx}, so it is possible to carry out information about boundary layer pattern [3]. The visualized temperature distribution, is correlated whit property of the external flow and the ones of the body. If the body is cooler than air, it will be characterized by an increasing of temperature due to tangential conduction, followed by a first decrement in the flow acceleration zones. After this, temperature starts to decrease quickly due to the change of h_x and finally it starts to rise. The area of temperature trend inversion is usually characterized by a fluid-dynamics transition (laminar to turbulent) or aerodynamic bubble. The maximum gradient of temperature is generally located in a very small area close to the antinode of the profile. Experimental tests have be done to visualize this pattern using different samples, materials and measurement chains. Only the more representative are illustrated in this work [4]. The goal is to search for a numerical validation to have more information about this phenomenon.

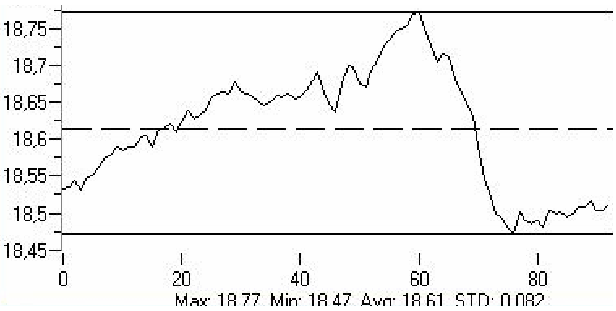

Fig. 1: Classic temperature distribution on a wing

2 Theoretical issue

Reynold's analogy is not sufficient for an exhaustive analysis, it must be associated to the internal energy of the fluid flow that is strictly correlated with Mach number. Generally working with high Mach numbers (i.e. transonic flow or more) a direct reading of energy can be done [9]. This energy in slow subsonic flows (i.e. very low Mach number) is not sufficient to produce a remarkable heat gradient on the body surface. Frequently this problem can be resolved in two different way: the first one, called "*active technique*", needs to heat the body surface artificially, the other ("*passive technique*") wants the fluid flow heated. Passive technique is less intrusive for the physical phenomenon.

The most used method to monitor motion field by thermographic measurement is an active – stationary called *heated-thin-foil technique* [5-6-7-8]. It consists of heating the observed body by metallic sheets, like copper or similar, or by printed circuit boards. By monitoring temperature and knowing thermal flow produced by Joule's effect, it is possible to find thermal convection coefficient between body and fluid using the energy balance expression:

$$h = \frac{\left(\Phi_j - \Phi_{cond.lat} - \Phi_{rad}\right)}{\left(T - T_\infty\right)} \tag{4}$$

An alternative way to proceed is to use transient flow condition and passive set-up. It is represented by the *thin skin technique*. In this case the body is considered with reduced thermal capacity and resistance. Under determined assumption it is possible to suppose an instantaneous heat transfer inside the body until equilibrium and consequently it's possible to neglect internal conduction.

Referring to the general equation of heat conduction without thermal source, this condition is represented by:

$$\Phi = c \cdot \rho \cdot e \cdot \frac{\partial T}{\partial t} \tag{5}$$

As a result of this relation, it's sufficient to monitor the temporal development of superficial temperature to obtain informations about convection coefficient [11]:

$$h = \frac{\left(c \cdot \rho \cdot e \cdot \dfrac{\partial T}{\partial t}\right)}{\left(T_\infty - T\right)} \tag{6}$$

In another way it is possible to admit hypothesis of *semi-infinite body* in which is theoretically expectable the thermal pattern due to conduction. Body temperature is representable by the following relation [12]:

$$\mathrm{T} = \frac{1}{2 \cdot \sqrt{\pi \cdot \mathrm{a} \cdot \mathrm{t}}} \cdot \int_{-\infty}^{\infty} \mathrm{f}(\mathrm{x'}) \cdot e^{-\frac{(x - x^*)^2}{4 \cdot a \cdot t}} \cdot \mathrm{dx'} \tag{7}$$

The last two hypothesis expect flow heating, enforcing a passive technique work.

3 Experimental test

Experimental tests are used to investigate in qualitative way boundary layer pattern of an airfoil. The goal is to connect it to thermal maps in slow subsonic flow condition and to compare direct vision with passive technique. Two type of tests have been conducted. The first one adopts an open circuit wind tunnel where temperature pattern can be considered constant. The second set uses a closed circuit wind tunnel where passive method is adopted using the own heating of the wind tunnel. Thermographic system used is an high sensitivity CCD thermocamera, manufactured by Stress Photonics, the Deltatherm 1560 system.

3.1 Open circuit wind tunnel

An aluminium wing profile with length of 153 mm and chord of 100 mm was tested in a slow subsonic wind tunnel with a test section of 400*400 mm. Function typology is by aspiration. Aluminium is choose for its internal high conductivity. Temperature and wind speed were monitored by a thermal resistor and a Pitot's tube positioned inside the tunnel. Measured temperature gradient was minor than 0,01 K, therefore temperature is considered as a constant for the specific issue.

A first test was done covering the profile with black paint to avoid reflection effects and different emissivity values effects on its surface. The wing profile was fixed by one end using a 0 degrees angle of attach on the test section of the wind tunnel.

Acquired thermographic images show that convection thermal exchange between flow and body propagate very quickly. Due to aluminium high conductivity inside the body the temperature pattern shows only a temperature increment with thickness profile decrement (figure 2).

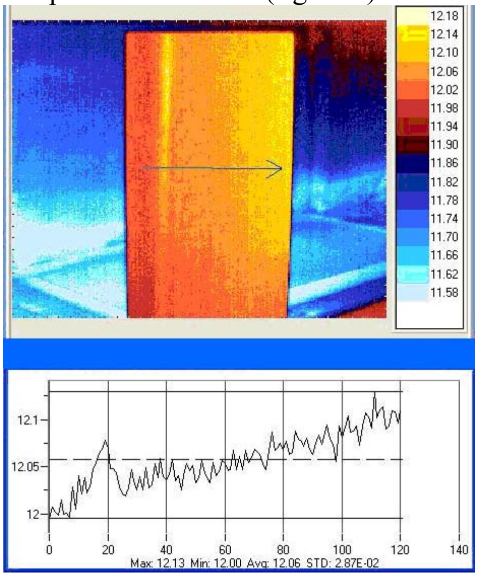

Fig.2 Temperature distribution for aluminium airfoil

To take out high conductivity effects, the profile was covered with a film of Mylar® with a thickness of 12 μm. Mylar® is an insulation, strong and durable polyester film. Thermal properties of Mylar® are summarized in the table 1.

Table 1: Typical Value of Mylar® film

Property	Typical Value	Unit
Specific Heat	1172	J/kg *K
Thermal Conductivity	1.5 E-04	W/mm* K

To avoid reflection effects, it was also covered by a black film, with an high emissivity coefficient.

The following image, obtained for a flow velocity of 23 m/s, shows that temperature pattern is the typical previously described: temperature grown up and the decrease to the transition zone.

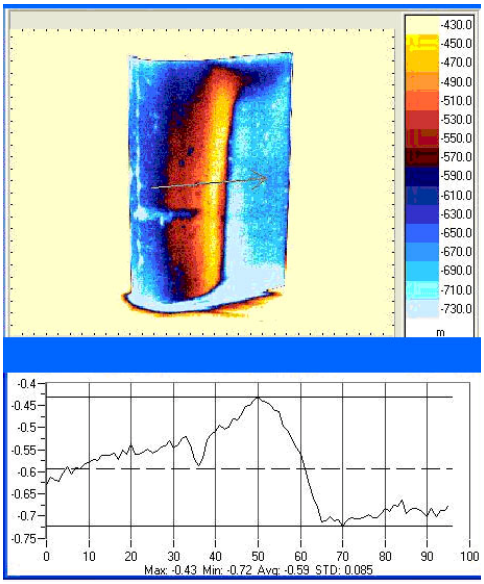

Fig. 3 Temperature distribution for aluminium airfoil black painted and Mylar® 12 μm covered in open circuit wind tunnel

To confirm results another set of tests was accomplished using an angle of attach of 7,5 degrees clockwise. Acquired thermographic images show a boundary layer pattern shifted compared to the one obtained for 0 degree angle of incidence.

Rotating of 7,5 degrees counter clockwise the profile, acquired thermographic images show a different boundary layer pattern, in fact there isn't temperature gradient.

3.2 Closed circuit wind tunnel

To validate and confirm the techniques, airfoil was tested also in a different subsonic wind tunnel with a test section of 2200x2200mm and recirculating flow. During the wind tunnel run, air temperature increases by friction due the interaction with the honey-comb in the tunnel. Tests were accomplished by using passive technique. Flow velocity during the test was 42 m/s.

Also in this case wing profile was covered by a film of Mylar® with a thickness of 12 μm and a black film on it. It was positioned in the wind tunnel using 0 degrees angle.

In this case airfoil is hotter than fluid so that when fluid arrives to the leading edge of the body starts to cool for tangential conduction phenomena [8]. After fluid detaches, superficial temperature became constant.

The gradient of temperature is the one that appears when boundary layer detaches. In this case it is reversed if compared with the previous because the body was cooled by the flow (Figure 3).

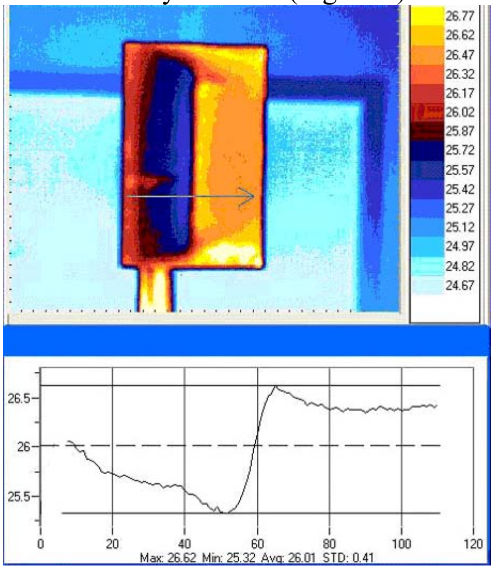

Fig.4 Temperature distribution for airfoil tested in closed circuit wind tunnel

4 Numerical approach

An other way to approach the problem is the numerical analysis, the so called CFD.

If the results obtained with the calculus are close to the experimental data, it's possible to validate them and to use them to explore not only the temperature distribution over the surface of the body but also the flow field surrounding the wing.

Different analytical models were used to determine the best solution both in a steady and in an unsteady state.

Furthermore, a very fine grid must be used for the analysis, the local flow separation phoenomenon involves the heat exchange behaviour. Figure 5 shows the mesh adopted with a thin boundary layer and a finest zone to resolve the wake.

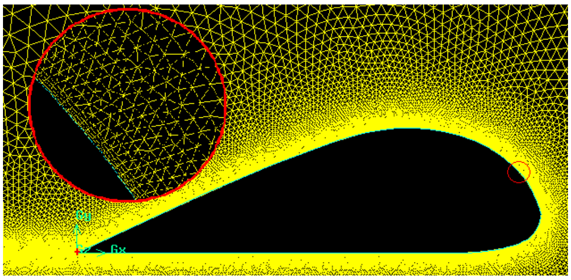

Fig. 5: Discretization of the model

4.1 The model adopted

The main approaches selected to simulate the process are two: the first and less costly method is based on the RANS model; then a LES model was used to understand better the small scale phenomena.

The first set of the analyses is executed using the k-ε realizable model with wall function and enabling the viscous heating option. The inlet boundary condition is imposed using the experimental data condition such as the velocity, the temperature, the pressure and the turbulence (the length scale has the magnitude of the honeycomb cells).

The thermal equilibrium was reached assigning an adiabatic condition to the surface of the body, *i.e.* neglecting temperature sources. The physical properties of the Mylar are assigned to the wall of the wing.

The low Mach number and the very small temperature gradient justify an incompressible fluid formulation.

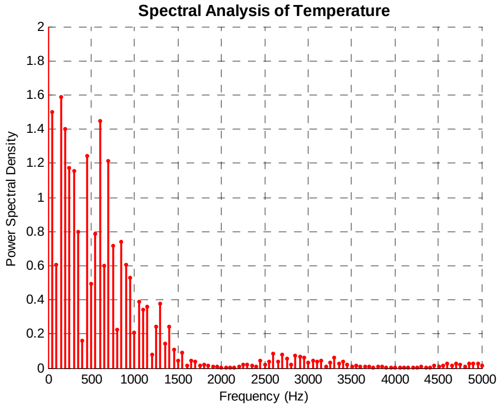

Fig. 6: Temperature Spectral Density at a node

The second set of the analyses adopt the LES model. A time step of 5e-05 sec. was used and the results are observed for a period of 0.02 seconds. The spectrum of the unsteady behaviour of the flow is showed in figure 6. The main events occur at a frequency from 0 to 2000 Hz, so the time step used can describe the flow.

4.2 The results

All the analyses are performed using a commercial CFD package, a Fluent Inc. product.

The results are evaluated with the aid of the flow field contour map and by plotting the temperature distribution along the upper side of the wing profile.

The RANS method calculation is presented in figure 7. The diagram in figure 8 shows a positive gradient of temperature starting from the leading edge to the “hump” according with the experimental data. Then the temperature decreases up to the trailing edge of the wing. The two equation based on models, such as k-ε, can’t resolve completely the flow separation and the transition between laminar and turbulence boundary layer [13].

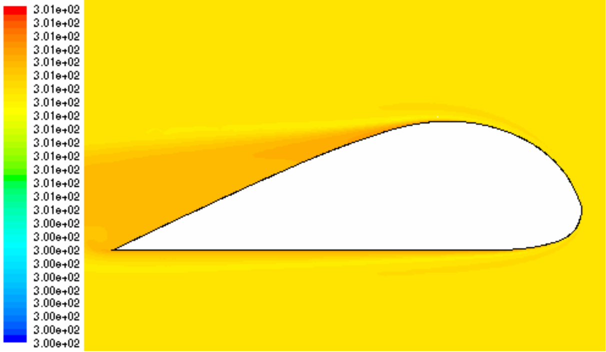

Fig 7: Temperature distribution (RANS model)

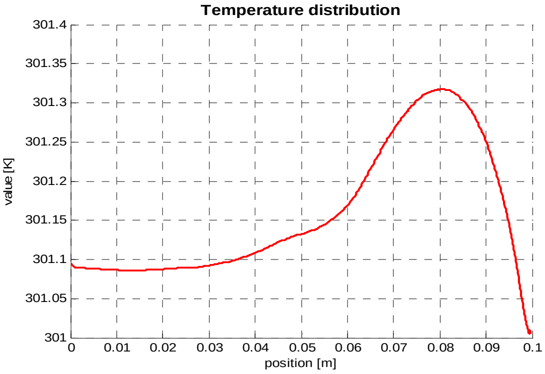

Fig. 8: Temperature distribution along the suction side for the RANS solution

A modified turbulence viscosity model [14] could be used to overcome this occurrence. This could be done by using the experimental observation and the Reynolds Analogy in order to switch the heat transfer coefficient between a laminar or a turbulent value.An other, but more expensive way to explore the heat exchange is the LES model. The following figures and diagrams show the results obtained for two different time steps.

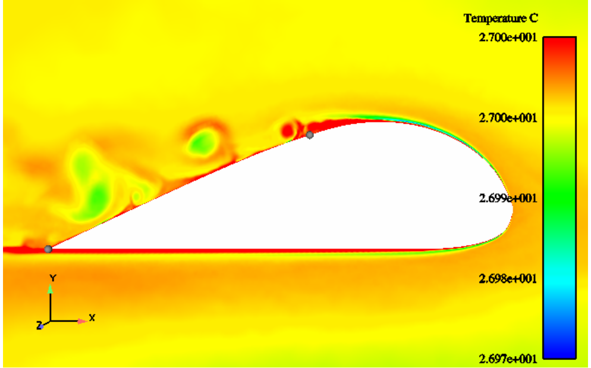

Fig. 9: Temperature field at 0.038 sec

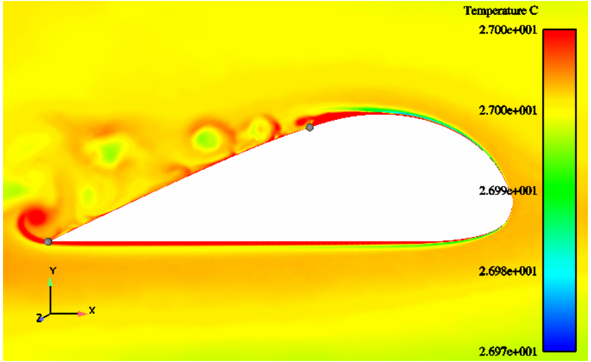

Fig. 10: Temperature field at 0.040 sec.

The leading edge temperature distribution is the same as the obtained one with the k-ε model. Afterwards some “picks” of temperature occur close to the zone at a greater vorticity. The turbulent heat exchange is thus greater than in laminar zone. Figure 9 and figure 10 show this occurrence.

Diagrams in figure 11 and 12 report the temperature variation along the chord at different time steps.

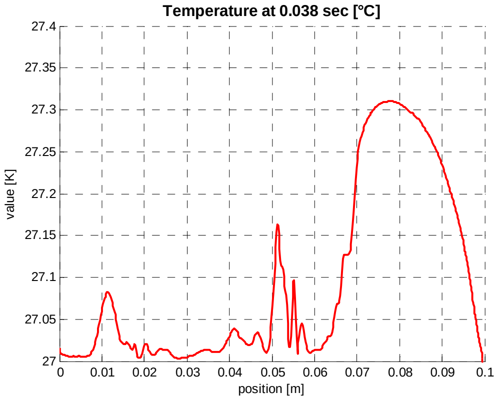

Fig. 11: Temperature distribution at 0.038 sec.

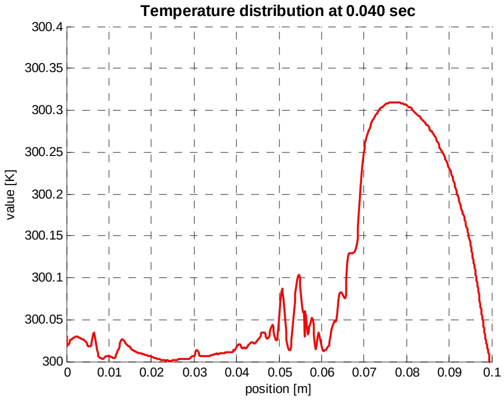

Fig. 12: Temperature distribution at 0.040 sec.

The last consideration can be done with the aid of the medium value obtained averaging all the results.

The temperature distribution along the chord of the wing is similar to the other analyses in the zone close to the leading edge. However, moving toward the trailing edge a small increase of temperature occurs (figure 13). This behaviour is more similar to the experimental results obtained.

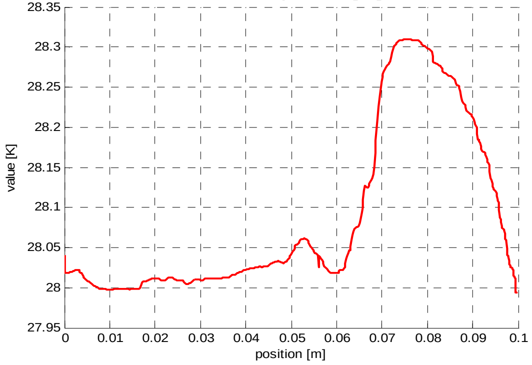

Fig. 13: Averaged temperature along the chord

Inside the wake the mean temperature contours differ from the ones obtained with the RANS method.

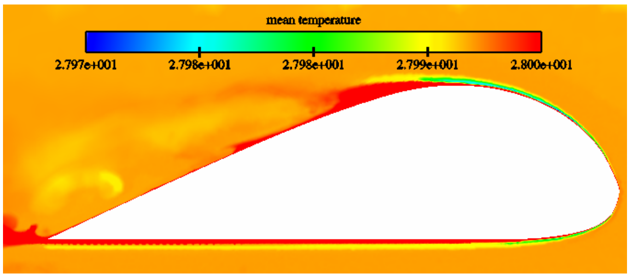

Fig. 14: Contours of Mean Temperature

Finally, both the averaged value and the time dependent solution are related to the total time of observation and to the sampling frequency.

5 Conclusion

Results explained on this paper, demonstrate that the high sensitivity thermographic technique can be used to obtain a fast qualitative evaluation of boundary layer also for low subsonic flow.

The difference between experimental and numerical data can be seen firstly in the slope of the initial ramp starting from the leading edge of the profile. The experimental value rises more slowly than the numerical data. This can be explained considering the one-dimensional thermographic images versus the bi-dimensional distribution of the numerical data. The models adopted show a good accordance with the experimental data in terms of macroscopic behaviour. To understand the small scale and unsteady events the LES approach is more reliable.

References:

[1] E. Gartenberg, A. S. Roberts Jr., Twenty-Five Years of Aerodynamics Research with Infrared Imaging, *Journal of Aircraft*, Vol.29, No2, March-April 1992

[2] F. Kreith, *Principi di Trasmissione del Calore* , Liguori Editore,1988

[3] I. Barducci, *Trasmissione del Calore*, Vol.1, Milano 1991, Editoriale ESA

[4]M. Malerba, A. Salviuolo, G.L. Rossi, Qualitative fluid-dynamic analysis of wing profile by thermographic technique, *XIV A.I.VE.LA National Meeting,* November 2006.

[5] G. M. Carlomagno, L. De Luca, Infrared Thermography for Flow Visualization and Heat Transfer Measurement, *Workshop on: Stato dell'arte del rilevamento con Camere Termiche nella banda 8-14micron,* 1991, pp.191-219

[6]G. M. Carlomagno, G. Cardone, T. Astarita, Wall Heat Transfer in Static and Rotating 180° Turn Channels by Quantitative Infrared Thermography, *Rev. Gen. Therm*., 37, 1998, pp. 644-652, Elsevier Science, Paris.

[7]G. Cardone, T. Astarita, Thermofluidynamics Analysis of the Flow in a Sharp 180° Turn Channel, *Experimental Thermal and Fluid Science,* 20, 2000, pp. 188-200, Elsevier Science.

[8]T. Astarita, G. Cardone, G. M. Carlomagno, C. Meola, A survey on Infrared Thermography for Convective Heat Transfer Measurement, *Optics & Laser Technology*, 2001, Elsevier Science

[9]J. E. Lamar, Flow Visualization Techniques Used at High Speed by Configuration Aerodynamics Wind-Tunnel-Test Team, *NASA report*, No TM-2001-210848, April 2001

[10]D. L. Balageas, A-M. Bouchardy, Application of Infrared Termography in Fluid Mechanics", Lecture Series on "Measurement Techniques, *Von Karman Institute for Fluid Dynamics*, 1993-05

[11]M. Carbonaro, P. Maggiorana, R. Marsili, An innovative methodology in the characterization of halogen lamp as reference source for Heat Flux Sensors calibration, *Measurement Science and Technologies*, June 02, Institute of Physics Publishing

[12]H. S. Carslaw, J.C. Jaeger, *Conduction of Heat in Solids*, Second Edition, Oxford Science Pubblications,1990

[13]J. H. Fersiger, M. Peric, *Computational Methods for Fluid Dynamics,* Springer, 2002

[14] H.K. Versteeg, W. Malalasekera, *An Introduction to Computational Fluid Dynamics*, Longman, 1995